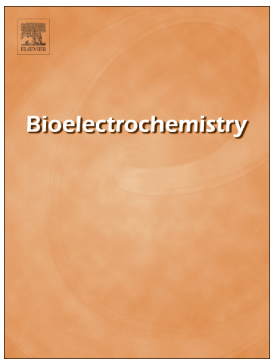

Double strand DNA-based determination of menadione using a Fe3O4 nanoparticle decorated reduced graphene oxide modified carbon paste electrode

Maryam Hosseini Ghalehno, Mohammad Mirzaei, Masoud Torkzadeh-Mahani

PII: S1567-5394(18)30176-2
DOI: doi:10.1016/j.bioelechem.2018.07.014
Reference: BIOJEC 7192

To appear in: *Bioelectrochemistry*

Received date: 20 April 2018
Revised date: 18 July 2018
Accepted date: 18 July 2018

Please cite this article as: Maryam Hosseini Ghalehno, Mohammad Mirzaei, Masoud Torkzadeh-Mahani , Double strand DNA-based determination of menadione using a Fe3O4 nanoparticle decorated reduced graphene oxide modified carbon paste electrode. Biojec (2018), doi:10.1016/j.bioelechem.2018.07.014

Double strand DNA -based determination of menadione using a Fe_3O_4 nanoparticle decorated reduced graphene oxide modified carbon paste electrode

Maryam Hosseini Ghalehno[a,b], Mohammad Mirzaei[a], Masoud Torkzadeh-Mahani [c*]

[a]Department of Chemistry, Shahid Bahonar University of Kerman, Kerman, Iran.

[b]Young Research Society, Shahid Bahonar University of Kerman, Kerman, Iran.

[c]Department of Biotechnology, Institute of Science, High Technology and Environmental Sciences, Graduate University of Advanced Technology, Kerman, Iran.

*Corresponding author at Department of Biotechnology, Institute of Sciences, High Technology and Environmental Sciences, Graduate University of Advanced Technology, Kerman, Iran

Tel/fax: +98 3433776617 E-mail address: mtmahani@gmail.com

Abstract

In this work an electrochemical label free DNA biosensor (ds-DNA) for the determination of menadione (MD) was developed. The biosensor was constructed using a modified nanocomposite consisting of Fe_3O_4 nanoparticles decorated reduced graphene oxide (Gr) on a carbon paste electrode (CPE). Scanning electron microscope (SEM), energy dispersive X-ray (EDAX) and Fourier transform infrared (FT-IR) spectroscopy confirmed the structure of the synthesized nanocomposites (electrode composition). The Gr-Fe_3O_4 nanocomposites formed a sensitive layer with large surface area. Electrochemical studies revealed that modification of the electrode surface with ds-DNA and Gr- Fe_3O_4 nanocomposite significantly increases the oxidation peak currents and reduces the peak potentials of MD. Under the optimum conditions, calibration curve was linear in the range of 0.3 – 100.0 nM with a detection limit of 0.13 nM. The relative standard deviation for 50.0 nM was 3.90 % (n=5). The proposed biosensor was successfully applied to the determination of MD.

Keywords: DNA biosensor, Carbon paste electrode, Menadione, Nanocomposite

1. Introduction

Menadione (vitamin K_3, 2-methyl- 1,4-naphthoquinone, MD) is a synthetic pro-vitamin which has shown antihemorrhagic and anti-inflammatory activity because of the presence of the quinone function group in its structure [1]. Recently, much interest has been generated in MD due to its potential as a clinically useful antitumor agent.

MD has also been shown to inhibit the growth of a variety of rodent and human tumor cells in vitro [2, 3]. In the human tumor cell soft-agar cloning assay, menadione inhibits the growth of several human solid tumor cell types [4]. A variety of analytical methods have been developed in order to determine menadione levels in different sample matrices including polarography [5], stripping voltammetry [6], fluorimetry [7] and kinetic measurement [8]. Menadione was also determined by high-performance liquid chromatography [9-11] and flow injection analysis (FIA) [12, 13] using photometric [11] and fluorimetric [9, 10, 13] detection. However, these methods usually suffer from some disadvantages with regard to cost and selectivity, use of organic solvents, complex sample preparation procedures and long analysis time.

In the last years, DNA electrochemical biosensors have attracted much attention because of their low cost, high sensitivity, rapid response time, and good selectivity as well as their capacity for instrument miniaturization [14-16]. Up to now, various types of DNA electrochemical biosensors using a broad range of nanomaterials such as Au-NPs [17], carbon nanotubes (CNTs) [18] and graphene [19] have been used to improve the sensitivity and stability of DNA biosensors. As one of the most important transition metal oxides, iron oxide (Fe_3O_4) is a promising supercapacitor electrode material because of its low cost, high abundance, biocompatibility, low toxicity and good electrochemical performance [20, 21]. Nanocomposites based on Fe_3O_4 have been fabricated to prepare conductive materials [22]. For instance, Fe_3O_4-graphene composites have been developed as electrode materials, triggering increased interest as a result of the positive synergistic effects between Fe_3O_4 and graphene [23, 24].

Graphene (Gr) is a monolayer of sp^2 hybridized carbon atoms packed into a dense honeycomb crystal structure. This configuration provides the material with extraordinary properties, such as prominent thermal stability [25], superior electronic conductivity [26, 27], remarkable structural flexibility [28, 29], high specific surface area [30], and widespread potential applications [31] in nanoscience and nanotechnology. Therefore, considering physicochemical properties of the Gr and its low costs, it is suggested that Gr sheets could be an ideal matrix for the growing and anchoring of a large number of functional substances.

In this study, a sensitive method was developed for detection of menadione based on the ds-DNA-coated carbon paste electrode modified with Fe_3O_4 nanoparticles decorated reduced graphene oxide. We have constructed a modified carbon paste ds-DNA electrode by the Gr-Fe_3O_4

nanocomposite (Scheme. 1). The Gr-Fe_3O_4 nanocomposite was directly synthesized from graphene oxide (GO) and iron chloride ($FeCl_3$, $6H_2O$) in the presence of hydrazine hydrate.

2. Experimental

2.1. Material and methods

All voltammetric experiments were performed with Autolab PGSTAT 204, potentiostat/galvanostat connected to a three-electrode cell composed of a platinum wire as the auxiliary electrode, Ag/AgCl/KCl (saturated) as the reference electrode and carbon paste electrode as the working electrode. All pH measurements were carried out using a Metrohm 827 pH meter (Herisau, Switzerland) supplied with a combination glass reference electrode.

The menadione powder was purchased from Merck. We have prepared 0.1 M stock solution of menadione by dissolving an appropriate amount of the powder in distiled water; the soultion was then sonicated for 10 minutes and stored at 4 °C. Double-strand salmon sperm DNA (ds-DNA) was purchased from Sigma (St. Louis, USA). A 1.0 mg mL^{-1} stock solution of the DNA was prepared in Tris–HCl buffer (pH=7.4) and kept frozen.

Graphene oxide was purchased from Sigma; $FeCl_3.6H_2O$, ascorbic acid, hydrazine hydrate, sodium dihydrogen phosphate, sodium acetate, acetic acid, phosphoric acid and hydrochloric acid were purchased from Merck (Darmstadt, Germany).

2.2. Preparation of Gr–Fe_3O_4 nanocomposites

Gr–Fe_3O_4 nanocomposites were synthesized according to previous work [32]. Briefly, about 0.036 g Gr oxide was dispersed in 40 mL deionized water. Subsequently, 0.270 g $FeCl_3.6H_2O$ and 0.528 g ascorbic acid were added to the beaker, forming a homogenous solution by ultra sonication. Then, 10 mL hydrazine hydrate were added to the mixture with vigorous stirring. Then, the black solution was transferred into a 50 mL Teflon-lined stainless steel autoclave and heated at 180 °C for 8 h. After cooling to room temperature, solid precipitate was separated by centrifugation and washed three times with deionized water and alcohol, respectively. Finally, the Gr–Fe_3O_4 composites were obtained by drying at 60 °C under vacuum for 12 h.

2.3. Fabrication of the DNA electrochemical biosensor

Several electrodes with the different percentage of the Gr–Fe_3O_4 nanocomposites were prepared and assayed for determination of MD. The results showed that an electrode containing 2.0 w/w% Gr–Fe_3O_4 nanocomposites has excellent sensitivity for the determination of MD.

After the modification of the electrode, the ds-DNA was immobilized on the Gr–Fe_3O_4/CPE as described in the literature [33]. It was performed by adding 10 mL of 0.5 M acetate buffer solution (pH 4.8) containing 0.1 M DNA. Subsequently, the ds-DNA was stirred for 400 s after immersing Gr–Fe_3O_4/CPE and a 0.50 V potential was applied on the working electrode. The electrode was then rinsed with acetate buffer (0.50 M, pH 4.8). Thus, a DNA-coated Gr–Fe_3O_4/CPE was obtained.

2.4. Electrochemical detection

Electrochemical detection was performed by immersing ds-DNA-coated Gr–Fe_3O_4/CPE into 10 mL phosphate buffer (0.1 M, pH=8.0) containing different concentrations of MD, and the solution was stirred at an open circuit system for different times (accumulation step). The electrode was then rinsed with distilled water and placed in10 mL of 0.40 M phosphate buffer solution (pH 7.00). The electrochemical responses of the accumulated MD were recorded by scanning the potential range from -300 mV to 300 mV using the differential pulse voltammetry with the scan rate as 100 mV s^{-1} (stripping step). All the analytical results were the average values of three parallel measurements. The design concept of the assay system is displayed in Scheme 1.

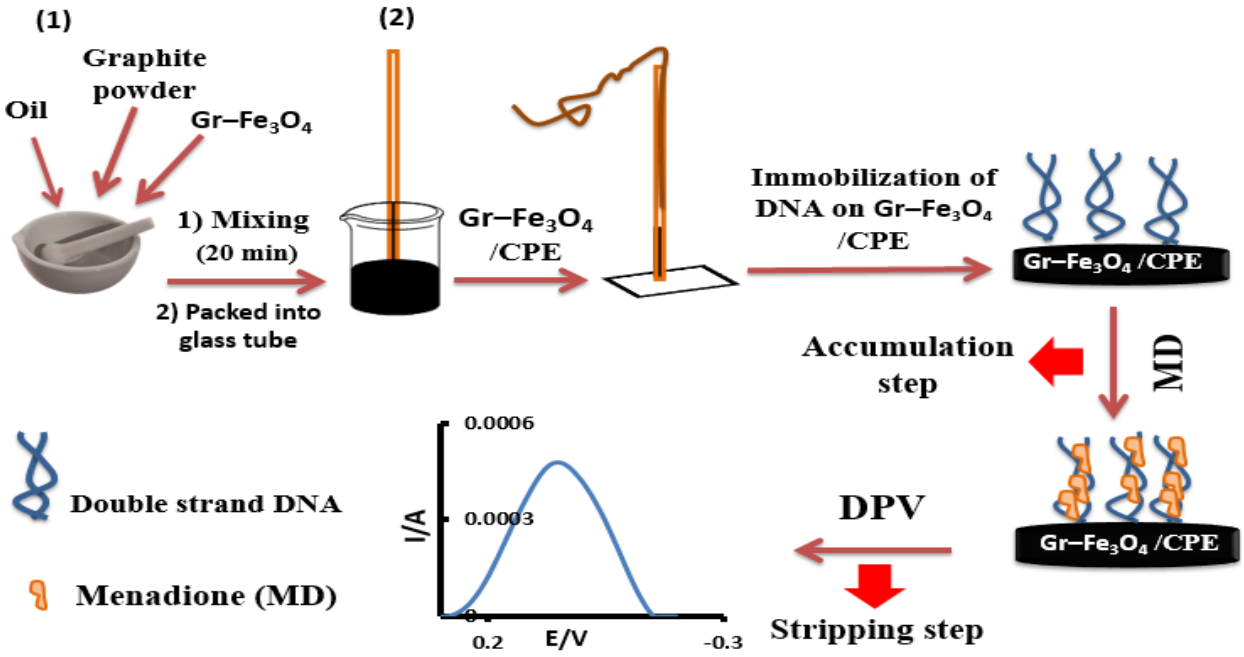

Schematic. 1. Schematic diagram of the construction of DNA sensor for the detection of menadione

3. Results and discussion

3. 1. Interaction between MD and the dsDNA in solution

CV voltammogramms of MD in phosphate buffer (0.10 M, pH 7.40) recorded in the absence and presence of the dsDNA, were shown in Fig. 1. As can be seen, after adding the dsDNA and incubating for 5 min the peak current of MD decreased with a positive shift in the peak potential (130 mV). Such results may be attributed to one of the following two factors: (i) the non-conducting DNA could block the electron transfer between MD and electrode surface or (ii) the DNA–MD complex formed was electrochemically inactive [33]. If the electron transfer was blocked, then the current should decrease (relative to that of the clean electrode) but no peak shift would be expected**.** In the presence of DNA, the current is mainly due to unbound species, since the diffusion rate of the DNA-bound species is small [34].

So, this observed decrease in the anodic current of MD is attributed to the decrease in the unbound MD concentration due to the formation of the MD–DNA complex which is a consequence of DNA addition. Furthermore, the peak potential shifted to more positive value after interaction with the dsDNA. As mentioned in the literature (Lu etal.,2004), a negative shift in peak potential is a characteristic of an electrostatic mode interaction between DNA and

desired specie while a positive shift indicates an interaction of intercalative mode. Accordingly, the positive shift in the peak potential of MD is attributed to a characteristic behavior of the intercalation of MD into the DNA double helix. According to these observations, it seems that the decrease of peak current of MD after addition of the dsDNA is caused by the intercalation of MD into the bulky, slowly diffusing DNA, which results in a considerable decrease in the apparent diffusion coefficient.

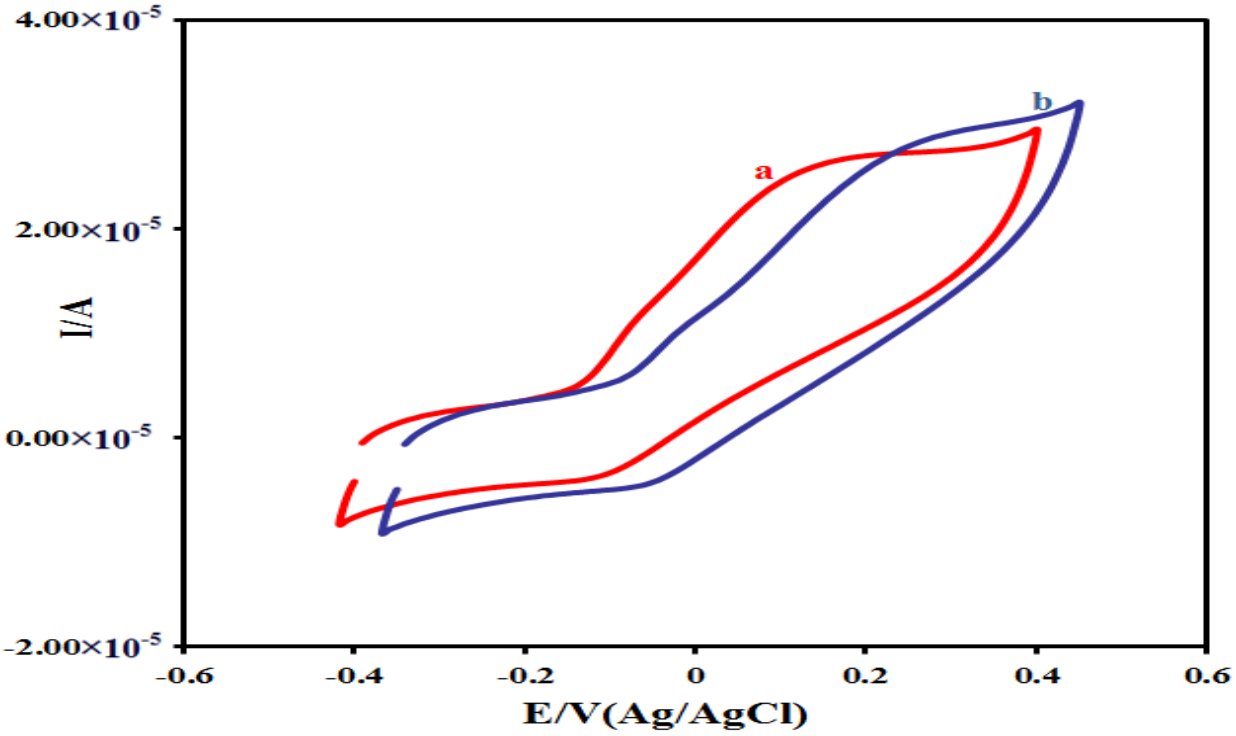

Figure. 1. CV voltammograms of 50.0 n M MD at CPE in 0.1 M phosphate buffer of pH 7.4 in the absence of the dsDNA (a) and in the presence the dsDNA (b). Incubation time, 5 min.

3.2. Characterization of Gr–Fe_3O_4 nanocomposite

The surface homogeneity and morphology of the Gr–Fe_3O_4 nanocomposite has been investigated using scanning electron microscopy. As seen in Fig. 2.a and b, the SEM image clearly demonstrated the relatively uniform distribution of the Fe_3O_4 nanoparticle on the reduced graphene oxide with the dimension range of 1-500 nm.

The EDAX spectrum reveals Fe (III) signal on the surface of the graphene oxide (Fig. 2.c). Only the presence of carbon, oxygen, and iron peaks in the EDAX spectrum indicates a purity synthesis.

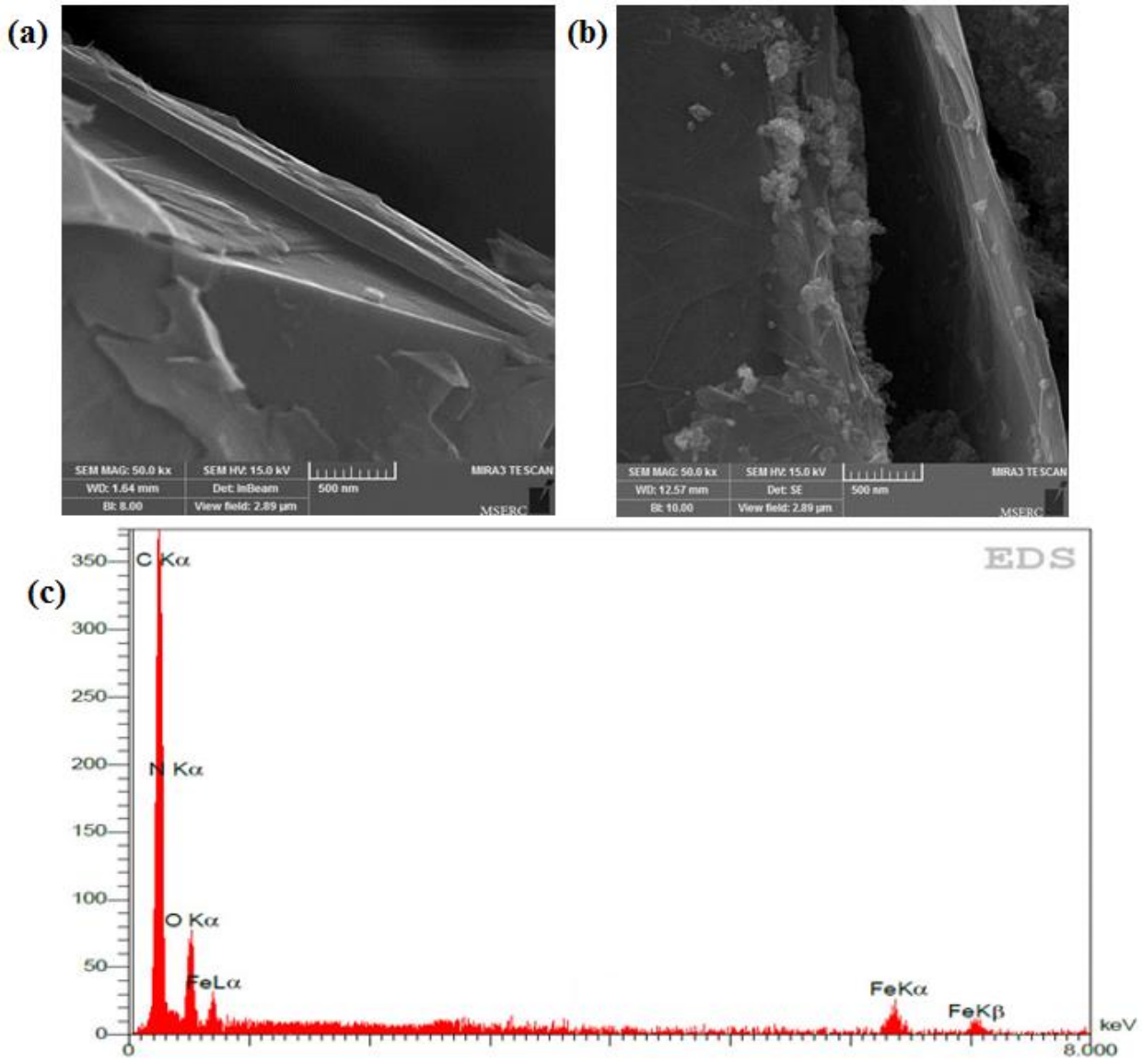

Figure. 2. SEM images from surface of (a) GO/CPE and (b) Gr–Fe_3O_4/CPE, (c) EDAX patterns of Gr–Fe_3O_4 nanocomposite

FT-IR also indicated the chemical structure of the prepared composite. As seen in Fig. 3.a, the FT-IR spectrum of the Gr oxide represented the existence of the C-O stretching vibration of epoxide (1163 cm^{-1}), tertiary C-OH groups stretching (3416.20cm^{-1}), and C=O stretching of carbonyl and carboxyl groups (1726 cm^{-1}). The synthesized Fe_3O_4 nanoparticles (Fig. 3.b) can be observed from the occurrence of a strong absorption band in the FT-IR spectrum which encompasses the characteristic wavenumber of 625 cm^{-1}. This pattern corresponds to the Fe–O bonds, which is reported to belong to bulk magnetite [35]. FT-IR spectrum of Gr–Fe_3O_4 shows

that the peaks at 625 and 560 cm^{-1} were denoted to the stretching vibrations of Fe–O–Fe, expounding the presence of iron oxide. Compared with Gr oxide, the intensity of absorption bands due to alkoxy, carboxy and carbonyl/carboxy bonds decreased. The results suggested that the decoration of Gr with Fe_3O_4 had been performed successfully.

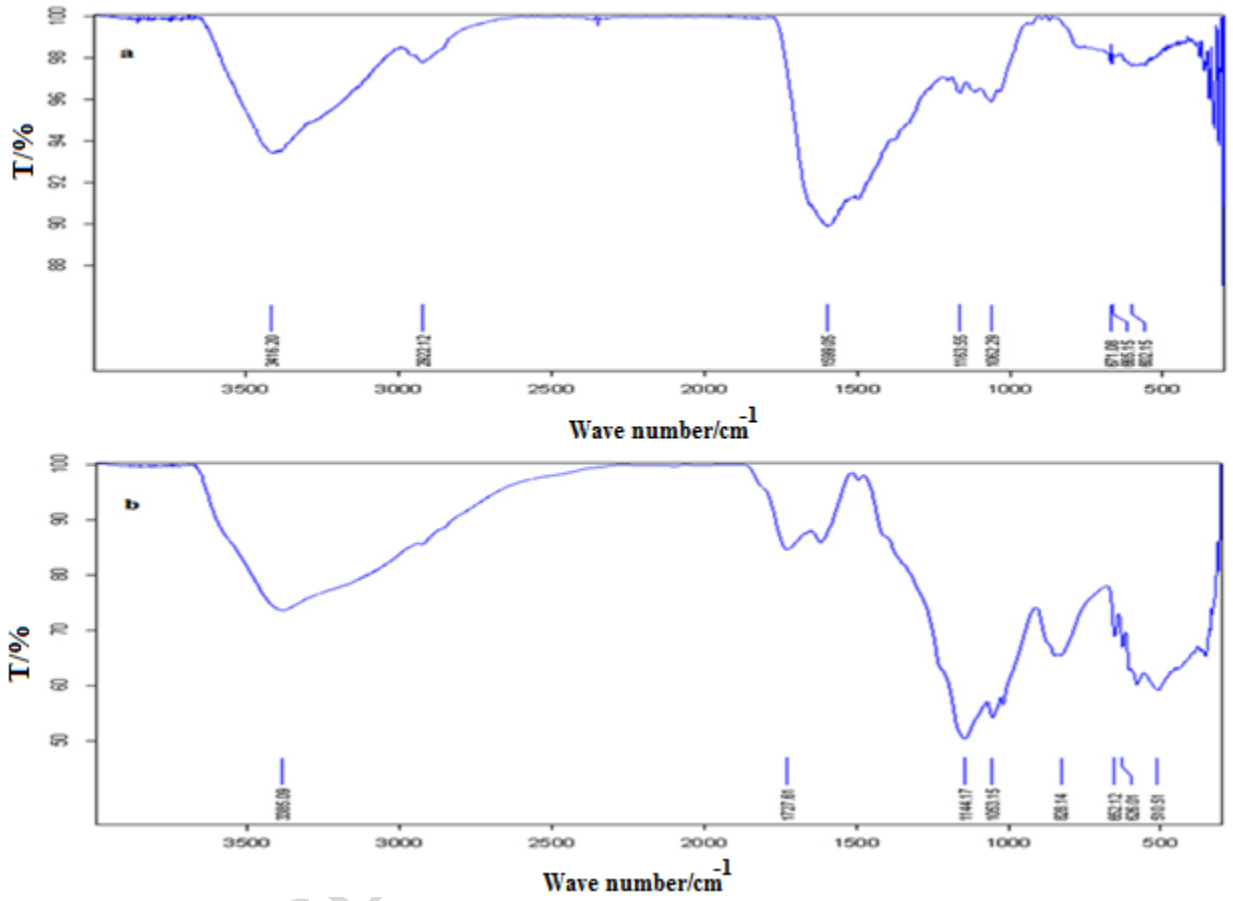

Figure. 3. FT-IR spectra for GO oxide (a) and Gr–Fe_3O_4 nanocomposite (b).

3.3. Electrochemical characterization of different modified electrodes

Cyclic voltammetry (CV) was used for the study of DNA immobilization on the Gr–Fe_3O_4/CPE surfaces. In the present study, the $Fe(CN)_6^{3-}/Fe(CN)_6^{4-}$ redox couple, (0.05 M K_3 Fe $(CN)_6$ and 0.05 M K_4 Fe $(CN)_6$ in 0.01 M PBS and 0.1 M NaCl) was used as the redox probe. The function of this indicator is based on the electrostatic repulsion of the redox couple and also on the negatively charged DNA phosphate backbone. As shown in Fig. 4, both the peak currents at Gr–Fe_3O_4/CPE were improved more than bare CPE. Since the relative electrochemically active surface area has increased in Gr–Fe_3O_4/CPE, the peak current increased.

After the immobilization of DNA at the surface of the Gr–Fe_3O_4/CPE both the peak currents were dramatically diminished. Due to electrostatic repulsion, the negatively charged phosphate backbone of the DNA prevented the redox couple [Fe (CN) $_6^{3-}$/Fe (CN) $_6^{4-}$] from reaching the electrode surface, leading to a decrease in the oxidation and reduction signals.

Consequently, the difference between the CV profiles for these electrodes enables detection of the immobilization of the ds-DNA on the surface of the Gr–Fe_3O_4/CPE.

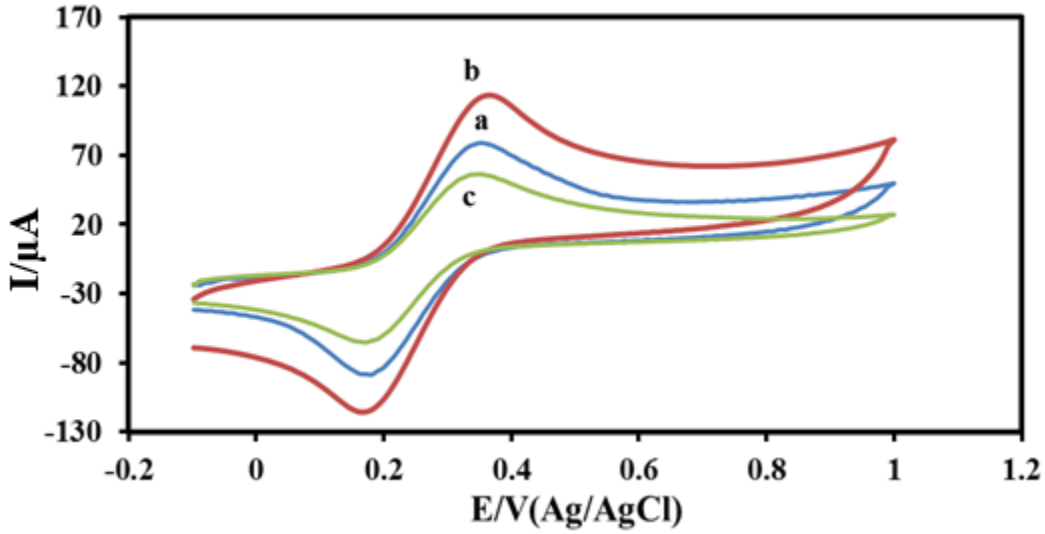

Figure. 4. Cyclic voltammograms of (a) bare CPE, (b) Gr- Fe_3O_4 /CPE and (c) ds DNA-coated Gr–Fe_3O_4 /CPE in 0.05 M $K_3Fe(CN)_6$ and 0.05 M $K_4Fe(CN)_6$ and 0.1 M NaCl. Conditions: potential range -0.1 to 1.0 V and scan rate 100 mV s^{-1}.

3.4. Determination of menadione

3.4.1. Voltammetric behavior of MD at surface of DNA-coated Gr-Fe_3O_4/CPE

Fig. 5 shows the DP voltammograms (DPVs) for 50.0 nM MD at CPE, Gr/CPE, Gr–Fe_3O_4/CPE and DNA-coated Gr–Fe_3O_4/CPE in phosphate buffer solution with accumulation medium of 0.10 M phosphate buffer pH 8.0, and stripping medium of 0.4 M phosphate buffer pH 7.0. There were poor oxidation peaks in the DPV responses of CPE. This indicates the slow electron transfer rate for the oxidation of MD at CPE. An obvious increase in the redox peak current of MD was observed in the DPV response of Gr/CPE, indicating the increase of electron transfer rate. Moreover, the enhanced peak current intensity was due to the special structure of Gr and large surface area of Gr/CPE. The above results indicate that Gr/CPE had better electrochemical activity. Fig. 5c demonstrates that Gr–Fe_3O_4/CPE can effectively increase the electro-oxidation of MD and

greatly improve the peak shape. This can mainly be attributed to its large surface area and low surface resistance. Fig. 5d indicated that the oxidation signal of MD at the DNA-coated Gr-Fe_3O_4/CPE was improved. The significant increase of the oxidation peak current suggested a preconcentration due to the adsorption of MD at the DNA-coated Gr-Fe_3O_4/CPE surface through a strong interaction with the immobilized DNA layer. Moreover, the intercalative binding of MD with the surface-confined DNA layer adsorbs and preconcentrates MD in the surface of the DNA-coated Gr-Fe_3O_4/CPE, resulting in the enhanced sensitivity.

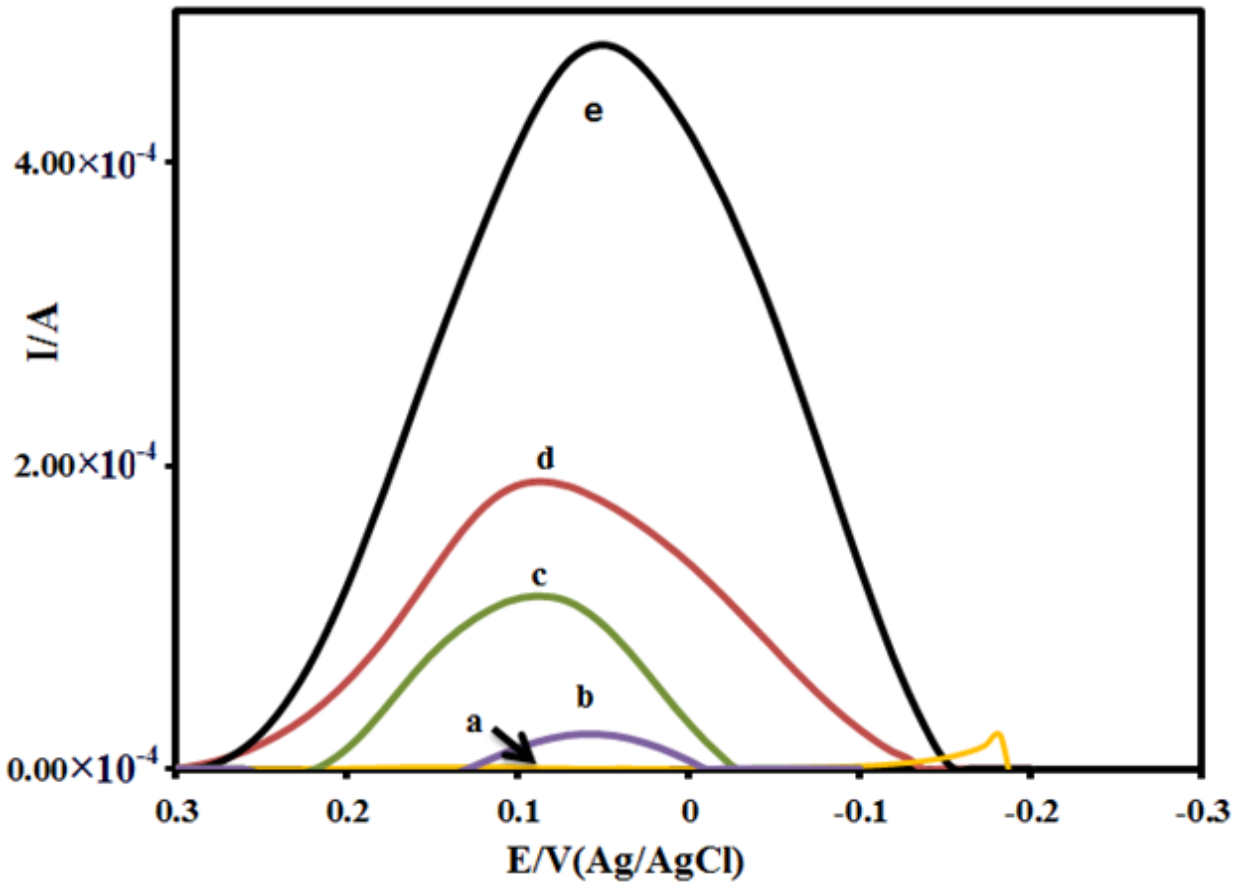

Figure. 5. DP voltammograms obtained in absence of MD (a) and after accumulation of MD on the surface of bare CPE (b), Gr-CPE (c), and Gr–Fe_3O_4 /CPE (d) in comparison with DNA-coated Gr–Fe_3O_4/CPE (e). Conditions: accumulation medium 0.10 M phosphate buffer pH 8.0, accumulation time 15 min, stripping medium 0.4 M phosphate buffer pH 7.0.

3.4.2. Effect of scan rate

The effect of the potential scan rate (υ) on electrochemical properties of the ds-DNA/ Gr–Fe_3O_4/CPE was investigated by CV. Plots of the both anodic and cathodic peak currents (Ip) were

linearly dependent on υ in the range of 20.0–180.0 mVs^{-1} (Fig. S 1). The results showed that the anodic peak currents varied linearly with the scan rate (υ), confirming the adsorption process oxidation of MD in the range 20.0-180.0 mVs^{-1}. The linear regression equations for the redox process are written as $Ip_a = 1.21x + 4.28$; $R^2 = 0.98$ and $Ip_c = -0.82x - 39$; $R^2 = 0.97$.

3.4.3. Optimization of experimental conditions

Effects of concentration, pH and various supporting electrolytes (Britton–Robinson buffer, phosphate buffer) on the accumulation step were investigated on the oxidation of MD using the ds-DNA coated Gr–Fe_3O_4/CPE.

The maximal peak current of MD was obtained in phosphate buffer solution. Accumulation buffer was evaluated in phosphate buffer ranging from 2.0 to 10.0 pH values. As was shown in Fig. S. 2 a, the oxidation peak with the high current was obtained at pH = 8.0.

In addition, the concentration of accumulation buffer was evaluated at the concentration ranging from 0.05 to 0.5 M. As one can see in Fig. S. 2 b, the maximum signal was observed in 0.1 M of phosphate buffer and thus this concentration of buffer was selected as optimum.

The effect of stripping pH on the MD biosensor response was investigated in different types of buffers (Tris-HCl buffer, phosphate buffer, acetate buffer) with different concentrations of buffer (0.1- 0.6 M) and pH values ranging from 3.00 to 9.00. This result indicates that with using the phosphate buffer solution at pH 7.0 and 0.4 M concentration, Ip_a was maximum (Fig. S. 2 c, d). Therefore, in subsequent experiments, the stripping was carried out in 0.4 M phosphate buffer with pH 7.0.

The dependence of the anodic peak current of MD to the stirring time in the range of 4-15 min was investigated. The time of 15 min was chosen as the optimum accumulation time.

3.5. Analytical performance

DP voltammetry was adopted in the experiments, and the peak current of the oxidation wave of MD at 50 mV was used as the detecting signal. Fig. 6 shows the DPV response of the ds-DNA-coated Gr–Fe_3O_4/CPE for different MD concentrations, and a calibration curve for MD detection

with the proposed biosensor under the optimal experimental conditions. The calibration graph exhibits a linear relationship between the peak current at the ds-DNA-coated Gr–Fe_3O_4 /CPE and the MD concentration over the range of 0.3 – 100.0 nM. The linear equation was I (μA) =2.57 [MD] +198.5 with R^2=0.99 and the detection limit was 0.13 nM. The intercept of calibration curve was high due to increasing of residual peak current.

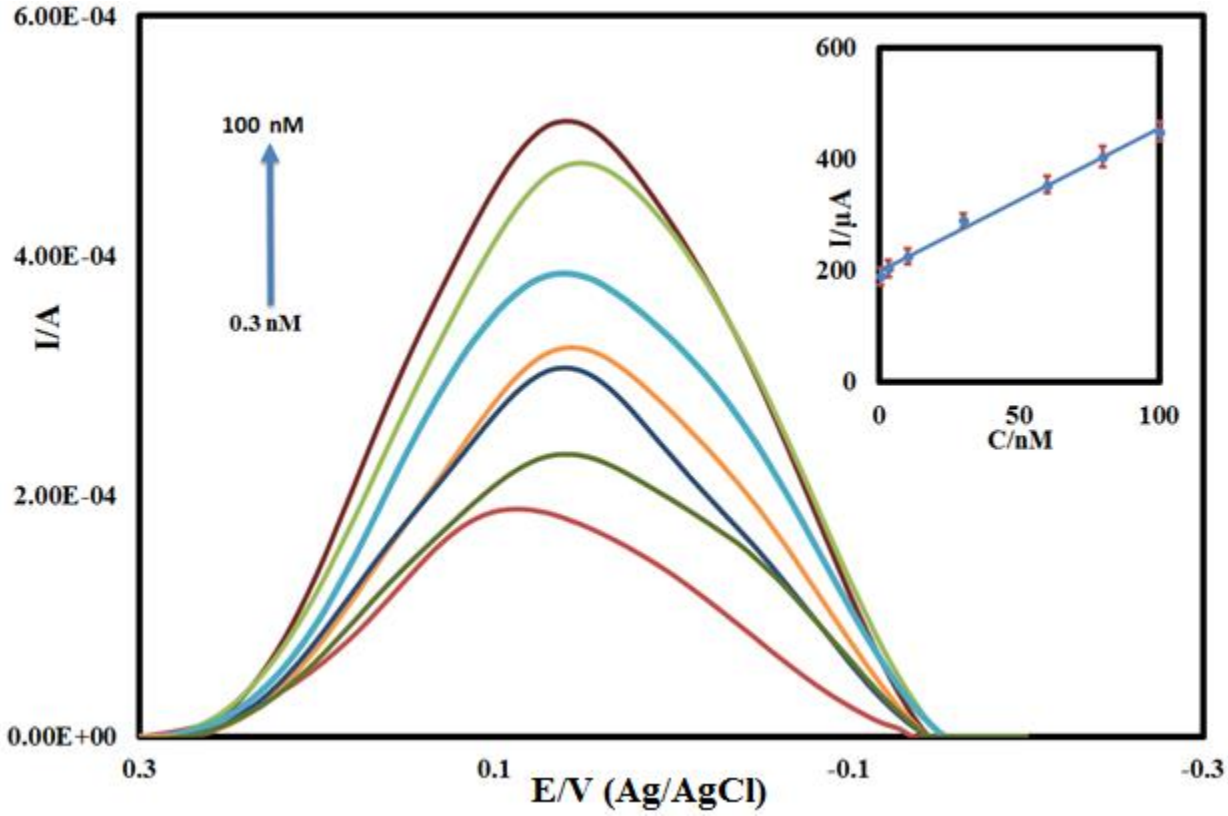

Figure. 6. DP voltammograms and calibration curve of MD obtained at DNA-coated Gr–Fe_3O_4 /CPE at different concentrations: 0.3, 3.0, 10.0, 30.0, 60.0, 80.0 and 100.0 nM. The linear equation obtained y =2.57 x +198.5 with R^2 = 0.99. Other conditions were the same as given in Fig.5.

3.6. Stability and reproducibility of MD biosensor

Stability of the DNA biosensor was investigated for one week. After keeping in refrigerator (4°C) for one week, the DNA biosensor was used to detect the same MD concentration (50.0 nM). The peak current only decreased 6.10 % of its initial current, demonstrating that the DNA biosensor had good stability.

The reproducibility of the DNA biosensor was tested by determining 50.0 nM of MD with five different DNA biosensors that were prepared independently. The relative standard deviation was 4.20% for five independent determinations. The experimental results indicated good reproducibility of the fabrication protocol.

Repeatability of the sensor was assessed by five replicate measurements (after accumulation on ds DNA-coated Gr–Fe_3O_4 /CPE at 50.0 nM of MD; the corresponding RSD was calculated to be 3.90%.

3.7. Real sample analysis

To further validate the applicability of the proposed biosensor for real sample analysis, it was employed to determine the concentration of MD in the human blood serum and urine sample.

For this purpose, healthy people's samples were prepared according to the literature with minor modifications [38]. Aliquots of the urine sample (1.0 mL) were spiked with given amounts of MD and then treated with 1.0 mL of methanol to precipitate the urine proteins. After stirring the sample for almost 30s, the precipitated proteins were separated by centrifugation at 6000 rpm for 15 min. The clear, protein-free supernatant layer was filtered through the 0.45 mm Millipore filter and diluted to 10 mL with 0.1 M phosphate buffer (pH=8.0).

One milliliter of the blood serum sample was transferred into each of the centrifuge tubes containing different known amounts of MD and then mixed well with 1.0 mL of methanol to precipitate the blood proteins. After centrifugation at 6000 rpm for 15 min and separation of the precipitated proteins, the clear supernatant layer was filtered through the 0.45 mm Millipore filter and then diluted to 10 ml with 0.1 M phosphate buffer (pH=8.0). For the determination of MD in each sample, the ds-DNA-coated Gr–Fe_3O_4/CPE was immersed into 10 mL of the prepared sample solution while stirring at an open circuit condition for 15 min (accumulation step). Then, in blank phosphate buffer solution (0.4 M, pH 7.0), DP voltammogram was recorded.

As shown in Table 1, the spiked recoveries are satisfactory and confirm that the proposed DNA-coated Gr–Fe_3O_4/CPE biosensor is applicable for determining MD in real sample assays.

Table. 1. Determination of MD in human serum and urine sample using the proposed biosensor.

Sample	Added(n M)	Found(n M)[a]	Recovery (%)
	0.0	0.0	-

Human serum	10.0	10.30±1.28	103
	30.0	30.54±0.90	101.8
	50.0	49.73±1.5	99.46
	0.0	0.0	-
Urine sample	10.0	9.92±0.85	99.2
	30.0	30.21±1.09	100.7
	50.0	50.28±0.9	100.56

[a]Mean ± standard deviation (n = 3).

3.8. Comparison with other methods

Table 2 compares some response characteristics of the proposed biosensor with some of the analytical characteristics of the previously reported MD voltammetric sensors. As one can see, our proposed biosensor not only shows a reasonably low LOD (0.13 nM) and wider linear range comparable to or better than the other methods, but also is simple, relatively cheap and flexible.

Table. 2. Comparison of the presented method with some methods currently reported for the determination of MD.

Method	Linear range (μM)	LOD (μM)	Ref
Electrochemical Reduction/Glassy carbon electrode	7.0 –560.0 and 600.0–2550.0	1.66 and 5.53	[36]
Differential Pulse Polarographic /Dropping mercury electrode	0.6 -10.0	0.3	[4]
voltammetric determination/Glassy carbon electrode	4.0×10^{-1} – 90.0	1.4×10^{-2}	[37]
DNAsensor	0.3×10^{-3}- 100.0 $\times10^{-3}$	0.13×10^{-3}	This work

4. Conclusions

In summary, a simple method was described for the construction of the biosensor based on the immobilization of ds-DNA in the Gr-Fe_3O_4/CPE surface. The MD biosensor exhibited a low detection limit, fast response, good operational stability and reproducibility. The Gr-Fe_3O_4 nanocomposite can effectively provide large specific area and good conductivity for MD oxidation. Since this biosensor is simple and low cost, the possible application of this approach to clinical analysis is the subject of further studies.

Acknowledgment

This work was supported by grants from the Research Council of Shahid Bahonar University of Kerman and Graduate University of Advanced Technology of Kerman.

References:

[1] M.S. Elgawish, C. Shimomai, N. Kishikawa, K. Ohyama, M. Wada,N. Kuroda, Development and validation of the first assay method coupling liquid chromatography with chemiluminescence for the simultaneous determination of menadione and its thioether conjugates in rat plasma, Chemical research in toxicology. 26 (2013) 1409-1417.

[2] M. Cioroi, C. Georgescu,D. Tutunaru, The Quantification of Menadione as Nutritional Supplement in Feedingstuffs, Romanian Biotechnological Letters. 20 (2015) 10431-10438.

[3] F. Demirkaya-Miloglu, Y. Kadioglu,O. Senol, GC-FID and HPLC-DAD Methods for the Determination of Menadione Sodium Bisulphite Directly and by Converting Menadione Sodium Bisulphite to Menadione in Pharmaceutical Preparation, Iranian journal of pharmaceutical research: IJPR. 13 (2014) 353.

[4] S.A. Akman, F. Kusu, K. Takamura, R. Chlebowski,J. Block, Differential pulse polarographic determination of plasma menadione, Analytical biochemistry. 141 (1984) 488-493.

[5] T. Bjornsson, Disposition and function of vitamin K and vitamin K antagonists, Effects of Drugs on Nutrition (Roe DA, and Campbell TC, eds). Marcel Dekker, Inc. (1982) 114-128.

[6] J.-C. Vire, N.A. El Maali, G. Patriarche,G. Christian, Square-wave adsorptive stripping voltammetry of menadione (vitamin K3), Talanta. 35 (1988) 997-1000.

[7] J.B. Nevado, M.G. Laguna, Spectrofluorimetric determination of vitamin K3, Analyst. 123 (1998) 287-290.

[8] M.I. Helaleh, Simple kinetic method for assay of menadione in pharmaceuticals, Journal of AOAC International. 80 (1997) 756-761.

[9] A. Speek, J. Schrijver,W. Schreurs, Fluorimetric determination of menadione sodium bisulphite (vitamin K3) in animal feed and premixes by high-performance liquid chromatography with post-column derivatization, Journal of Chromatography A. 301 (1984) 441-447.

[10] S.M. Billedeau, Fluorimetric determination of vitamin k 3 (menadione sodium bisulfite) in synthetic animal feed by high-performance liquid chromatography using a post-column zinc reducer, Journal of Chromatography A. 472 (1989) 371-379.

[11] R. Laffi, S. Marchetti,M. Marchetti, Normal-phase liquid chromatographic determination of menadione in animal feeds, Journal-Association of Official Analytical Chemists. 71 (1988) 826-828.

[12] N.M. Rizk, Potentiometric determination of menadione (vitamin K3), Microchim Acta. 138 (2002) 53-58.

[13] Q. He, Z. Wang, X. Cao, H. CHEN,Y. KE, Determination of menadione sodium bisulfite in pharmaceutical preparations by flow-injection on-line photochemical spectrofluorometry, Analytical sciences. 17 (2001) 1209-1212.

[14] Y. Ding, Q. Wang, F. Gao,F. Gao, Highly sensitive and selective DNA biosensor using a dumbbell-shaped bis-groove binder of bi-acetylferrocene ethylenediamine complex as electrochemical indicator, Electrochim. Acta. 106 (2013) 35-42.

[15] K.-J. Huang, Y.-J. Liu, H.-B. Wang,Y.-Y. Wang, A sensitive electrochemical DNA biosensor based on silver nanoparticles-polydopamine@ graphene composite, Electrochim. Acta. 118 (2014) 130-137.

[16] M.H. Ghalehno, M. Mirzaei,M. Torkzadeh-Mahani, Aptamer-based determination of tumor necrosis factor α using a screen-printed graphite electrode modified with gold hexacyanoferrate, Microchimica Acta. 185 (2018) 165.

[17] L. Li, C. Ma, Q. Kong, W. Li, Y. Zhang, S. Ge, M. Yan,J. Yu, A 3D origami electrochemical immunodevice based on a Au@ Pd alloy nanoparticle-paper electrode for the detection of carcinoembryonic antigen, Journal of Materials Chemistry B. 2 (2014) 6669-6674.

[18] H.-P. Peng, Y. Hu, P. Liu, Y.-N. Deng, P. Wang, W. Chen, A.-L. Liu, Y.-Z. Chen,X.-H. Lin, Label-free electrochemical DNA biosensor for rapid detection of mutidrug resistance gene based on Au nanoparticles/toluidine blue–graphene oxide nanocomposites, Sens Actuators B Chem. 207 (2015) 269-276.

[19] C. Jiang, T. Yang, K. Jiao,H. Gao, A DNA electrochemical sensor with poly-l-lysine/single-walled carbon nanotubes films and its application for the highly sensitive EIS detection of PAT gene fragment and PCR amplification of NOS gene, Electrochim. Acta. 53 (2008) 2917-2924.

[20] G.-Y. Mao, W.-J. Yang, F.-X. Bu, D.-M. Jiang, Z.-J. Zhao, Q.-H. Zhang, Q.-C. Fang,J.-S. Jiang, One-step hydrothermal synthesis of Fe_3O_4@ C nanoparticles with great performance in biomedicine, Journal of Materials Chemistry B. 2 (2014) 4481-4488.

[21] P.R. Kumar, Y.H. Jung, K.K. Bharathi, C.H. Lim,D.K. Kim, High capacity and low cost spinel Fe_3O_4 for the Na-ion battery negative electrode materials, Electrochim. Acta. 146 (2014) 503-510.

[22] M. Vinothkannan, C. Karthikeyan, A.R. Kim,D.J. Yoo, One-pot green synthesis of reduced graphene oxide (RGO)/Fe_3O_4 nanocomposites and its catalytic activity toward methylene blue dye degradation, Spectrochimica Acta Part A: Molecular and Biomolecular Spectroscopy. 136 (2015) 256-264.

[23] S. Erogul, S.Z. Bas, M. Ozmen,S. Yildiz, A new electrochemical sensor based on Fe_3O_4 functionalized graphene oxide-gold nanoparticle composite film for simultaneous determination of catechol and hydroquinone, Electrochim. Acta. 186 (2015) 302-313.

[24] W. Zhang, J. Zheng, J. Shi, Z. Lin, Q. Huang, H. Zhang, C. Wei, J. Chen, S. Hu,A. Hao, Nafion covered core–shell structured Fe 3 O 4@ graphene nanospheres modified electrode for highly selective detection of dopamine, Anal Chim Acta. 853 (2015) 285-290.

[25] A.A. Balandin, S. Ghosh, W. Bao, I. Calizo, D. Teweldebrhan, F. Miao,C.N. Lau, Superior thermal conductivity of single-layer graphene, Nano letters. 8 (2008) 902-907.

[26] K.S. Novoselov, Z. Jiang, Y. Zhang, S. Morozov, H.L. Stormer, U. Zeitler, J. Maan, G. Boebinger, P. Kim,A.K. Geim, Room-temperature quantum Hall effect in graphene, Sci. 315 (2007) 1379-1379.

[27] K.S. Novoselov, A.K. Geim, S. Morozov, D. Jiang, M. Katsnelson, I. Grigorieva, S. Dubonos, Firsov,AA, Two-dimensional gas of massless Dirac fermions in graphene, Nat. 438 (2005) 197-200.

[28] D.A. Dikin, S. Stankovich, E.J. Zimney, R.D. Piner, G.H. Dommett, G. Evmenenko, S.T. Nguyen,R.S. Ruoff, Preparation and characterization of graphene oxide paper, Nat. 448 (2007) 457-460.

[29] C. Lee, X. Wei, J.W. Kysar,J. Hone, Measurement of the elastic properties and intrinsic strength of monolayer graphene, Sci. 321 (2008) 385-388.
[30] A. Peigney, C. Laurent, E. Flahaut, R. Bacsa,A. Rousset, Specific surface area of carbon nanotubes and bundles of carbon nanotubes, Carbon. 39 (2001) 507-514.
[31] C. Rao, K. Biswas, K. Subrahmanyam,A. Govindaraj, Graphene, the new nanocarbon, Journal of Materials Chemistry. 19 (2009) 2457-2469.
[32] J. Su, M. Cao, L. Ren,C. Hu, Fe3O4–graphene nanocomposites with improved lithium storage and magnetism properties, The Journal of Physical Chemistry C. 115 (2011) 14469-14477.
[33] Y. Wang, Y. Ni,S. Kokot, Voltammetric behavior of complexation of salbutamol with calf thymus DNA and its analytical application, Analytical biochemistry. 419 (2011) 76-80.
[34] T.W. Welch, H.H. Thorp, Distribution of metal complexes bound to DNA determined by normal pulse voltammetry, The Journal of Physical Chemistry. 100 (1996) 13829-13836.
[35] H. Bagheri, A. Afkhami, M. Saber-Tehrani,H. Khoshsafar, Preparation and characterization of magnetic nanocomposite of Schiff base/silica/magnetite as a preconcentration phase for the trace determination of heavy metal ions in water, food and biological samples using atomic absorption spectrometry, Talanta. 97 (2012) 87-95.
[36] G. Ziyatdinova, E. Ziganshina,H. Budnikov, Electrochemical reduction and quantification of menadione in sodium dodecyl sulfate micellar media, Journal of Solid State Electrochemistry. 17 (2013) 2679-2685.
[37] Z. Zhang, J. Zhang, H. Zhang, J. Xu, Y. Wen,W. Ding, Characterization of PEDOT: PSS-reduced graphene oxide@ Pd composite electrode and its application in voltammetric determination of vitamin K 3, Journal of Electroanalytical Chemistry. 775 (2016) 258-266.

Highlights

- A simple method for the determination of Menadione is presented here.
- This approach takes advantage of an electrochemical DNA biosensor.
- Gr–Fe_3O_4 nanocomposite was used here as a modifier in the carbon paste electrode.
- The biosensor exhibits a low detection limit, fast response, and good precision.
- This strategy could be used for the measurement of Menadione in real samples.